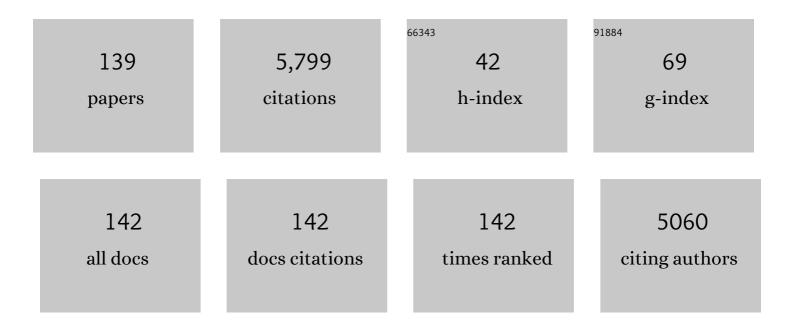
Guang-Rong Li

List of Publications by Year in descending order

Source: https://exaly.com/author-pdf/2237199/publications.pdf Version: 2024-02-01



#	Article	IF	CITATIONS
1	Pressure infiltration of molten aluminum for densification of environmental barrier coatings. Journal of Advanced Ceramics, 2022, 11, 145-157.	17.4	18
2	Difluorobenzylamine Treatment of Organolead Halide Perovskite Boosts the High Efficiency and Stability of Photovoltaic Cells. ACS Applied Materials & Interfaces, 2022, 14, 11388-11397.	8.0	11
3	The Bonding Formation during Thermal Spraying of Ceramic Coatings: A Review. Journal of Thermal Spray Technology, 2022, 31, 780-817.	3.1	20
4	Firstâ€principle calculations of CrN(200)/Ni(111) interface: Atomic structure, stability, and electronic properties. Surface and Interface Analysis, 2021, 53, 167-175.	1.8	5
5	Anion Exchangeâ€Induced Crystal Engineering via Hotâ€Pressing Sublimation Affording Highly Efficient and Stable Perovskite Solar Cells. Solar Rrl, 2021, 5, 2000729.	5.8	6
6	Formation of Intermetallic Compounds in a Cold-Sprayed Aluminum Coating on Magnesium Alloy Substrate after Friction Stir-Spot-Processing. Journal of Thermal Spray Technology, 2021, 30, 1464-1481.	3.1	3
7	Lead-Free Perovskite-Based Bifunctional Device for Both Photoelectric Conversion and Energy Storage. ACS Applied Energy Materials, 2021, 4, 7952-7958.	5.1	8
8	Organicâ€Inorganic Halide Perovskites: From Crystallization of Polycrystalline Films to Solar Cell Applications. Solar Rrl, 2020, 4, 1900200.	5.8	43
9	Effects of Powder Structure and Size on Gd2O3 Preferential Vaporization During Plasma Spraying of Gd2Zr2O7. Journal of Thermal Spray Technology, 2020, 29, 105-114.	3.1	5
10	Development of ScSZ Electrolyte by Very Low Pressure Plasma Spraying for High-Performance Metal-Supported SOFCs. Journal of Thermal Spray Technology, 2020, 29, 223-231.	3.1	17
11	Incorporated Guanidinium Expands the CH ₃ NH ₃ PbI ₃ Lattice and Enhances Photovoltaic Performance. ACS Applied Materials & Interfaces, 2020, 12, 43885-43891.	8.0	31
12	Catheter-integrated soft multilayer electronic arrays for multiplexed sensing and actuation during cardiac surgery. Nature Biomedical Engineering, 2020, 4, 997-1009.	22.5	175
13	Strain-Induced Cracking Behavior of Coating/Substrate Systems and Strain Tolerant Design for Thick Coatings. Coatings, 2020, 10, 1066.	2.6	2
14	Microstructure of Cross-Linked High Densification Network and Strengthening Mechanism in Cold-Sprayed Ti-6Al-4V Coating After Heat Treatment. Journal of Thermal Spray Technology, 2020, 29, 1054-1069.	3.1	7
15	Multifunctional Phosphorusâ€Containing Lewis Acid and Base Passivation Enabling Efficient and Moistureâ€Stable Perovskite Solar Cells. Advanced Functional Materials, 2020, 30, 1910710.	14.9	143
16	Lead-free perovskite [H ₃ NC ₆ H ₄ NH ₃]CuBr ₄ with both a bandgap of 1.43 eV and excellent stability. Journal of Materials Chemistry A, 2020, 8, 5484-5488.	10.3	20
17	Plasma spray–physical vapor deposition toward advanced thermal barrier coatings: a review. Rare Metals, 2020, 39, 479-497.	7.1	33
18	Dominant effect of oriented 2D pores on heat flux in lamellar structured thermal barrier coatings. Ceramics International, 2019, 45, 17029-17039.	4.8	3

#	Article	IF	CITATIONS
19	Pores Structure Change Induced by Heat Treatment in Cold-Sprayed Ti6Al4V Coating. Journal of Thermal Spray Technology, 2019, 28, 1199-1211.	3.1	30
20	Improved Environmental Stability and Solar Cell Efficiency of (MA,FA)PbI ₃ Perovskite Using a Wide-Band-Gap 1D Thiazolium Lead Iodide Capping Layer Strategy. ACS Energy Letters, 2019, 4, 1763-1769.	17.4	118
21	(C ₆ H ₅ NH ₃)Bil ₄ : a lead-free perovskite with >330 days humidity stability for optoelectronic applications. Journal of Materials Chemistry A, 2019, 7, 15722-15730.	10.3	33
22	Structure Evolution of Multiscaled Thermal Barrier Coatings During Thermal Exposure. , 2019, , 221-255.		4
23	Numerical simulation of the flow characteristics inside a novel plasma spray torch. Journal Physics D: Applied Physics, 2019, 52, 335203.	2.8	27
24	Flexible and Highly Durable Perovskite Solar Cells with a Sandwiched Device Structure. ACS Applied Materials & Interfaces, 2019, 11, 17475-17481.	8.0	13
25	Semiconductor polymeric graphitic carbon nitride photocatalysts: the "holy grail―for the photocatalytic hydrogen evolution reaction under visible light. Energy and Environmental Science, 2019, 12, 2080-2147.	30.8	803
26	Series and Parallel Module Design for Large-Area Perovskite Solar Cells. ACS Applied Energy Materials, 2019, 2, 3851-3859.	5.1	37
27	Durable TBCs with self-enhanced thermal insulation based on co-design on macro- and microstructure. Applied Surface Science, 2019, 483, 472-480.	6.1	61
28	Fatigue and Mechanical Behavior of Ti-6Al-4V Alloy with CrN and TiN Coating Deposited by Magnetic Filtered Cathodic Vacuum Arc Process. Coatings, 2019, 9, 689.	2.6	13
29	Combined effect of internal and external factors on sintering kinetics of plasma-sprayed thermal barrier coatings. Journal of the European Ceramic Society, 2019, 39, 1860-1868.	5.7	37
30	Green Solution-Processed Tin-Based Perovskite Films for Lead-Free Planar Photovoltaic Devices. ACS Applied Materials & Interfaces, 2019, 11, 3053-3060.	8.0	27
31	Plasma Spraying of Dense Ceramic Coating with Fully Bonded Lamellae Through Materials Design Based on the Critical Bonding Temperature Concept. Journal of Thermal Spray Technology, 2019, 28, 53-62.	3.1	15
32	Understanding of degradation-resistant behavior of nanostructured thermal barrier coatings with bimodal structure. Journal of Materials Science and Technology, 2019, 35, 231-238.	10.7	125
33	Cost effective perovskite solar cells with a high efficiency and open-circuit voltage based on a perovskite-friendly carbon electrode. Journal of Materials Chemistry A, 2018, 6, 8271-8279.	10.3	57
34	Microstructure and Transparent Super-Hydrophobic Performance of Vacuum Cold-Sprayed Al2O3 and SiO2 Aerogel Composite Coating. Journal of Thermal Spray Technology, 2018, 27, 471-482.	3.1	15
35	Imaging Slit Pores Under Delaminated Splats by WhiteÂLightÂInterference. Journal of Thermal Spray Technology, 2018, 27, 319-335.	3.1	20
36	Epitaxial growth and cracking of highly tough 7YSZ splats by thermal spray technology. Journal of Advanced Ceramics, 2018, 7, 17-29.	17.4	75

#	Article	IF	CITATIONS
37	Novel Method of Aluminum to Copper Bonding by Cold Spray. Journal of Thermal Spray Technology, 2018, 27, 624-640.	3.1	23
38	Epitaxial Growth and Cracking Mechanisms of Thermally Sprayed Ceramic Splats. Journal of Thermal Spray Technology, 2018, 27, 255-268.	3.1	20
39	Stage-sensitive microstructural evolution of nanostructured TBCs during thermal exposure. Journal of the European Ceramic Society, 2018, 38, 3325-3332.	5.7	32
40	Low-temperature SnO ₂ -modified TiO ₂ yields record efficiency for normal planar perovskite solar modules. Journal of Materials Chemistry A, 2018, 6, 10233-10242.	10.3	75
41	Improving Erosion Resistance of Plasma-Sprayed Ceramic Coatings by Elevating the Deposition Temperature Based on the Critical Bonding Temperature. Journal of Thermal Spray Technology, 2018, 27, 25-34.	3.1	5
42	Effect of Post-spray Shot Peening Treatment on the Corrosion Behavior of NiCr-Mo Coating by Plasma Spraying of the Shell–Core–Structured Powders. Journal of Thermal Spray Technology, 2018, 27, 232-242.	3.1	17
43	Gradient thermal cyclic behaviour of La2Zr2O7/YSZ DCL-TBCs with equivalent thermal insulation performance. Journal of the European Ceramic Society, 2018, 38, 1888-1896.	5.7	57
44	Hetero-Orientation Epitaxial Growth of TiO2 Splats on Polycrystalline TiO2 Substrate. Journal of Thermal Spray Technology, 2018, 27, 880-897.	3.1	7
45	Tuning Nucleation Sites to Enable Monolayer Perovskite Films for Highly Efficient Perovskite Solar Cells. Coatings, 2018, 8, 408.	2.6	9
46	Self-Enhancing Thermal Insulation Performance of Bimodal-Structured Thermal Barrier Coating. Journal of Thermal Spray Technology, 2018, 27, 1064-1075.	3.1	24
47	A comprehensive sintering mechanism for thermal barrier coatingsâ€Part III: Substrate constraint effect on healing of 2D pores. Journal of the American Ceramic Society, 2018, 101, 3636-3648.	3.8	31
48	(C ₆ H ₅ CH ₂ NH ₃) ₂ CuBr ₄ : A Lead-Free, Highly Stable Two-Dimensional Perovskite for Solar Cell Applications. ACS Applied Energy Materials, 2018, 1, 2709-2716.	5.1	73
49	Excellent Stability of Perovskite Solar Cells by Passivation Engineering. Solar Rrl, 2018, 2, 1800088.	5.8	61
50	Effect of Particle Size and Impact Velocity on Collision Behaviors Between Nano-Scale TiN Particles: MD Simulation. Journal of Nanoscience and Nanotechnology, 2018, 18, 4121-4126.	0.9	5
51	Strain/sintering co-induced multiscale structural changes in plasma-sprayed thermal barrier coatings. Ceramics International, 2018, 44, 14408-14416.	4.8	23
52	MD Simulation on Collision Behavior Between Nano-Scale TiO ₂ Particles During Vacuum Cold Spraying. Journal of Nanoscience and Nanotechnology, 2018, 18, 2657-2664.	0.9	5
53	Formation of Lamellar Pores for Splats via Interfacial or Sub-interfacial Delamination at Chemically Bonded Region. Journal of Thermal Spray Technology, 2017, 26, 315-326.	3.1	27
54	Sinteringâ€induced delamination of thermal barrier coatings by gradient thermal cyclic test. Journal of the American Ceramic Society, 2017, 100, 1820-1830.	3.8	74

#	Article	IF	CITATIONS
55	Colonization of Bacteria on the Surfaces of Cold-Sprayed Copper Coatings Alters Their Electrochemical Behaviors. Journal of Thermal Spray Technology, 2017, 26, 687-694.	3.1	4
56	Material nucleation/growth competition tuning towards highly reproducible planar perovskite solar cells with efficiency exceeding 20%. Journal of Materials Chemistry A, 2017, 5, 6840-6848.	10.3	149
57	Ultra-high open-circuit voltage of perovskite solar cells induced by nucleation thermodynamics on rough substrates. Scientific Reports, 2017, 7, 46141.	3.3	71
58	A comprehensive sintering mechanism for TBCsâ€Part II: Multiscale multipoint interconnectionâ€enhanced initial kinetics. Journal of the American Ceramic Society, 2017, 100, 4240-4251.	3.8	56
59	A comprehensive sintering mechanism for TBCsâ€Part I: An overall evolution with twoâ€stage kinetics. Journal of the American Ceramic Society, 2017, 100, 2176-2189.	3.8	81
60	Thermally Sprayed Large Tubular Solid Oxide Fuel Cells and Its Stack: Geometry Optimization, Preparation, and Performance. Journal of Thermal Spray Technology, 2017, 26, 441-455.	3.1	16
61	Edge Effect on Crack Patterns in Thermally Sprayed Ceramic Splats. Journal of Thermal Spray Technology, 2017, 26, 302-314.	3.1	34
62	Multiscale Pores in TBCs for Lower Thermal Conductivity. Journal of Thermal Spray Technology, 2017, 26, 1183-1197.	3.1	34
63	Super-Hydrophobic Surface Prepared by Lanthanide Oxide Ceramic Deposition Through PS-PVD Process. Journal of Thermal Spray Technology, 2017, 26, 398-408.	3.1	11
64	Strain-induced stiffness-dependent structural changes and the associated failure mechanism in TBCs. Journal of the European Ceramic Society, 2017, 37, 3609-3621.	5.7	45
65	Anomalous Epitaxial Growth in Thermally Sprayed YSZ and LZ Splats. Journal of Thermal Spray Technology, 2017, 26, 1168-1182.	3.1	15
66	Large-area high-efficiency perovskite solar cells based on perovskite films dried by the multi-flow air knife method in air. Journal of Materials Chemistry A, 2017, 5, 1548-1557.	10.3	115
67	Effect of Oxidation on the Bonding Formation of Plasma-Sprayed Stainless Steel Splats onto Stainless Steel Substrate. Journal of Thermal Spray Technology, 2017, 26, 47-59.	3.1	14
68	Sintering induced the failure behavior of dense vertically crack and lamellar structured TBCs with equivalent thermal insulation performance. Ceramics International, 2017, 43, 15459-15465.	4.8	62
69	Boundary layer tuning induced fast and high performance perovskite film precipitation by facile one-step solution engineering. Journal of Materials Chemistry A, 2017, 5, 18120-18127.	10.3	21
70	Evaporation of Droplets in Plasma Spray–Physical Vapor Deposition Based on Energy Compensation Between Self-Cooling and Plasma Heat Transfer. Journal of Thermal Spray Technology, 2017, 26, 1641-1650.	3.1	24
71	Comprehensive damage evaluation of localized spallation of thermal barrier coatings. Journal of Advanced Ceramics, 2017, 6, 230-239.	17.4	50
72	The Correlation of the TBC Lifetimes in Burner Cycling Test with Thermal Gradient and Furnace Isothermal Cycling Test by TGO Effects. Journal of Thermal Spray Technology, 2017, 26, 378-387.	3.1	50

#	Article	IF	CITATIONS
73	Suspension Plasma Sprayed Sr2Fe1.4Mo0.6O6â~δ Electrodes for Solid Oxide Fuel Cells. Journal of Thermal Spray Technology, 2017, 26, 432-440.	3.1	2
74	The Microstructure Stability of Atmospheric Plasma-Sprayed MnCo2O4 Coating Under Dual-Atmosphere (H2/Air) Exposure. Journal of Thermal Spray Technology, 2016, 25, 301-310.	3.1	5
75	La2NiO4+δ Infiltration of Plasma-Sprayed LSCF Coating for Cathode Performance Improvement. Journal of Thermal Spray Technology, 2016, 25, 392-400.	3.1	15
76	Formation of Cr2O3 Diffusion Barrier Between Cr-Contained Stainless Steel and Cold-Sprayed Ni Coatings at High Temperature. Journal of Thermal Spray Technology, 2016, 25, 526-534.	3.1	13
77	Thermally sprayed high-performance porous metal-supported solid oxide fuel cells with nanostructured La _{0.6} Sr _{0.4} Co _{0.2} Fe _{0.8} O _{3â^Î^} cathodes. lournal of Materials Chemistry A. 2016, 4. 7461-7468.	10.3	25
78	Nonâ€destructive production of natural environmentâ€adaptive superâ€hydrophobic hierarchical ceramic surface on a steel substrate. Micro and Nano Letters, 2016, 11, 680-683.	1.3	2
79	Relationship Between Designed Three-Dimensional YSZ Electrolyte Surface Area and Performance of Solution-Precursor Plasma-Sprayed La0.8Sr0.2MnO3â^î Cathodes. Journal of Thermal Spray Technology, 2016, 25, 1692-1699.	3.1	2
80	Facile and Scalable Fabrication of Highly Efficient Lead Iodide Perovskite Thin-Film Solar Cells in Air Using Gas Pump Method. ACS Applied Materials & Interfaces, 2016, 8, 20067-20073.	8.0	88
81	Understanding the Formation of Limited Interlamellar Bonding in PlasmaÂSprayed Ceramic Coatings Based on the Concept of Intrinsic Bonding Temperature. Journal of Thermal Spray Technology, 2016, 25, 1617-1630.	3.1	22
82	Hierarchical Formation of Intrasplat Cracks in Thermal Spray Ceramic Coatings. Journal of Thermal Spray Technology, 2016, 25, 959-970.	3.1	41
83	Microstructure of YSZ Coatings Deposited by PS-PVD Using 45ÂkW Shrouded Plasma Torch. Materials and Manufacturing Processes, 2016, 31, 1183-1191.	4.7	18
84	Plasma-Sprayed Thermal Barrier Coatings with Enhanced Splat Bonding for CMAS and Corrosion Protection. Journal of Thermal Spray Technology, 2016, 25, 213-221.	3.1	31
85	Microstructure and Properties of Porous Abradable Alumina Coatings Flame-Sprayed with Semi-molten Particles. Journal of Thermal Spray Technology, 2016, 25, 264-272.	3.1	13
86	Preparation of flexible perovskite solar cells by a gas pump drying method on a plastic substrate. Journal of Materials Chemistry A, 2016, 4, 3704-3710.	10.3	87
87	High Heat Insulating Thermal Barrier Coating Designed with Large Two-Dimensional Inter-lamellar Pores. Journal of Thermal Spray Technology, 2016, 25, 222-230.	3.1	12
88	WC-Co Composite Coating Deposited by Cold Spraying of a Core-Shell-Structured WC-Co Powder. Journal of Thermal Spray Technology, 2015, 24, 100.	3.1	13
89	Relationship Between Lamellar Structure and Elastic Modulus of Thermally Sprayed Thermal Barrier Coatings with Intra-splat Cracks. Journal of Thermal Spray Technology, 2015, 24, 1355-1367.	3.1	74
90	Mechanical property and wear performance dependence on processing condition for cold-sprayed WC-(nanoWC-Co). Applied Surface Science, 2015, 332, 80-88.	6.1	47

#	ARTICLE	IF	CITATIONS
91	Ceramic Nano-particle/Substrate Interface Bonding Formation Derived from Dynamic Mechanical Force at Room Temperature: HRTEM Examination. Journal of Thermal Spray Technology, 2015, 24, 720-728.	3.1	7
92	Healing of the Interface Between Splashed Particles and Underlying Bulk Coating and Its Influence on Isothermal Oxidation Behavior of LPPS MCrAlY Bond Coat. Journal of Thermal Spray Technology, 2015, 24, 611-621.	3.1	29
93	A TEM Study of the Microstructure of Plasma-Sprayed YSZ Near Inter-splat Interfaces. Journal of Thermal Spray Technology, 2015, 24, 907-914.	3.1	16
94	Atmospheric plasma-sprayed La _{0.8} Sr _{0.2} Ga _{0.8} Mg _{0.2} O ₃ electrolyte membranes for intermediate-temperature solid oxide fuel cells. Journal of Materials Chemistry A, 2015, 3, 7535-7553.	10.3	50
95	Characterization of Plasma Jet in Plasma Spray-Physical Vapor Deposition of YSZ Using a <80ÂkW Shrouded Torch Based on Optical Emission Spectroscopy. Journal of Thermal Spray Technology, 2015, 24, 1038-1045.	3.1	37
96	Morphology and Size Evolution of Interlamellar Two-Dimensional Pores in Plasma-Sprayed La2Zr2O7 Coatings During Thermal Exposure at 1300°C. Journal of Thermal Spray Technology, 2015, 24, 739-748.	3.1	48
97	Unexpected efficiency enhancement of flexible dye-sensitized solar cells by repeated outward bending. RSC Advances, 2015, 5, 85174-85178.	3.6	1
98	Behavioral study of flexible platinum counter electrodes under alternative bending conditions. RSC Advances, 2015, 5, 73155-73161.	3.6	1
99	Controlling grain size in columnar YSZ coating formation by droplet filtering assisted PS-PVD processing. RSC Advances, 2015, 5, 102126-102133.	3.6	11
100	Fabrication of Porous Stainless Steel by Flame Spraying of Semimolten Particles. Materials and Manufacturing Processes, 2014, 29, 1253-1259.	4.7	10
101	Effect of <scp><scp>TGO</scp></scp> Thickness on Thermal Cyclic Lifetime and Failure Mode of Plasmaâ€5prayed <scp><scp>TBC</scp><. Journal of the American Ceramic Society, 2014, 97, 1226-1232.</scp>	3.8	157
102	Microstructure, Mechanical Properties, and Two-Body Abrasive Wear Behavior of Cold-Sprayed 20Âvol.% Cubic BN-NiCrAl Nanocomposite Coating. Journal of Thermal Spray Technology, 2014, 23, 1181-1190.	3.1	14
103	Deposition Behavior of Semi-Molten Spray Particles During Flame Spraying of Porous Metal Alloy. Journal of Thermal Spray Technology, 2014, 23, 991-999.	3.1	20
104	Characterization of Nonmelted Particles and Molten Splats in Plasma-Sprayed Al2O3 Coatings by a Combination of Scanning Electron Microscopy, X-ray Diffraction Analysis, and Confocal Raman Analysis. Journal of Thermal Spray Technology, 2013, 22, 131-137.	3.1	27
105	Microstructure and Properties of Porous Ni50Cr50-Al2O3 Cermet Support for Solid Oxide Fuel Cells. Journal of Thermal Spray Technology, 2013, 22, 158-165.	3.1	6
106	Development of Particle Interface Bonding in Thermal Spray Coatings: A Review. Journal of Thermal Spray Technology, 2013, 22, 192-206.	3.1	86
107	Effect of Phase Transformation Mechanism on the Microstructure of Cold-sprayed Ni/Al-Al2O3 Composite Coatings during Post-spray Annealing Treatment. Journal of Thermal Spray Technology, 2013, 22, 398-405.	3.1	12
108	Modeling Thermal Conductivity of Thermally Sprayed Coatings with Intrasplat Cracks. Journal of Thermal Spray Technology, 2013, 22, 1328-1336.	3.1	45

#	Article	IF	CITATIONS
109	Microstructural and Mechanical Property Evolutions of Plasma-Sprayed YSZ Coating During High-Temperature Exposure: Comparison Study Between 8YSZ and 20YSZ. Journal of Thermal Spray Technology, 2013, 22, 1294-1302.	3.1	71
110	Evolution of Lamellar Interface Cracks During Isothermal Cyclic Test of Plasma-Sprayed 8YSZ Coating with a Columnar-Structured YSZ Interlayer. Journal of Thermal Spray Technology, 2013, 22, 1374-1382.	3.1	64
111	Critical bonding temperature for the splat bonding formation during plasma spraying of ceramic materials. Surface and Coatings Technology, 2013, 235, 841-847.	4.8	86
112	Improvement of Adhesion and Cohesion in Plasma-Sprayed Ceramic Coatings by Heterogeneous Modification of Nonbonded Lamellar Interface Using High Strength Adhesive Infiltration. Journal of Thermal Spray Technology, 2013, 22, 36-47.	3.1	39
113	Fabrication of Porous Molybdenum by Controlling Spray Particle State. Journal of Thermal Spray Technology, 2012, 21, 1032-1045.	3.1	12
114	Annealing Effect on the Intermetallic Compound Formation of Cold Sprayed Fe/Al Composite Coating. Journal of Thermal Spray Technology, 2012, 21, 571-577.	3.1	15
115	Isothermal Oxidation Behavior of NiCoCrAlTaY Coating Deposited by High Velocity Air-Fuel Spraying. Journal of Thermal Spray Technology, 2012, 21, 391-399.	3.1	36
116	Formation of Pore Structure and Its Influence on the Mass Transport Property of Vacuum Cold Sprayed TiO2 Coatings Using Strengthened Nanostructured Powder. Journal of Thermal Spray Technology, 2012, 21, 505-513.	3.1	15
117	Effect of Dispersed TiC Content on the Microstructure and Thermal Expansion Behavior of Shrouded-Plasma-Sprayed FeAl/TiC Composite Coatings. Journal of Thermal Spray Technology, 2012, 21, 689-694.	3.1	14
118	A Novel Plasma-Sprayed Durable Thermal Barrier Coating with a Well-Bonded YSZ Interlayer Between Porous YSZ and Bond Coat. Journal of Thermal Spray Technology, 2012, 21, 383-390.	3.1	45
119	Characterization of High-Temperature Abrasive Wear of Cold-Sprayed FeAl Intermetallic Compound Coating. Journal of Thermal Spray Technology, 2011, 20, 227-233.	3.1	19
120	Effect of Chemical Compositions and Surface Morphologies of MCrAlY Coating on Its Isothermal Oxidation Behavior. Journal of Thermal Spray Technology, 2011, 20, 121-131.	3.1	37
121	Influence of Deposition Temperature on the Microstructures and Properties of Plasma-Sprayed Al2O3 Coatings. Journal of Thermal Spray Technology, 2011, 20, 160-169.	3.1	44
122	Influence of TGO Composition on the Thermal Shock Lifetime of Thermal Barrier Coatings with Cold-sprayed MCrAlY Bond Coat. Journal of Thermal Spray Technology, 2010, 19, 168-177.	3.1	98
123	Microstructure and Electrochemical Behavior of a Structured Electrolyte/LSM-Cathode Interface Modified by Flame Spraying for Solid Oxide Fuel Cell Application. Journal of Thermal Spray Technology, 2010, 19, 311-316.	3.1	14
124	RELATION BETWEEN MICROSTRUCTURE AND THERMAL CONDUCTIVITY OF PLASMA-SPRAYED 8YSZ COATING. International Journal of Modern Physics B, 2010, 24, 3017-3022.	2.0	13
125	Development of a Ni/Al2O3 Cermet-Supported Tubular Solid Oxide Fuel Cell Assembled with Different Functional Layers by Atmospheric Plasma-Spraying. Journal of Thermal Spray Technology, 2009, 18, 83-89.	3.1	18
126	High-Temperature Erosion of HVOF Sprayed Cr3C2-NiCr Coating and Mild Steel for Boiler Tubes. Journal of Thermal Spray Technology, 2008, 17, 782-787.	3.1	58

#	Article	IF	CITATIONS
127	Thermal Failure of Nanostructured Thermal Barrier Coatings with Cold-Sprayed Nanostructured NiCrAlY Bond Coat. Journal of Thermal Spray Technology, 2008, 17, 838-845.	3.1	34
128	Formation of NiAl Intermetallic Compound by Cold Spraying of Ball-Milled Ni/Al Alloy Powder Through Postannealing Treatment. Journal of Thermal Spray Technology, 2008, 17, 715-720.	3.1	45
129	Influence of Powder Porous Structure on the Deposition Behavior of Cold-Sprayed WC-12Co Coatings. Journal of Thermal Spray Technology, 2008, 17, 742-749.	3.1	68
130	Influence of Microstructure on the Ionic Conductivity of Plasma-Sprayed Yttria-Stabilized Zirconia Deposits. Journal of the American Ceramic Society, 2008, 91, 3931-3936.	3.8	59
131	Microstructural Characterization of Cold-Sprayed Nanostructured FeAl Intermetallic Compound Coating and its Ball-Milled Feedstock Powders. Journal of Thermal Spray Technology, 2007, 16, 669-676.	3.1	55
132	Fabrication of Nano-TiO2 Coating for Dye-Sensitized Solar Cell by Vacuum Cold Spraying at Room Temperature. Journal of Thermal Spray Technology, 2007, 16, 893-897.	3.1	60
133	Characterization of Nanostructured WC-Co Deposited by Cold Spraying. Journal of Thermal Spray Technology, 2007, 16, 1011-1020.	3.1	97
134	Influence of Silver Doping on Photocatalytic Activity of Liquid-Flame-Sprayed-Nanostructured TiO2 Coating. Journal of Thermal Spray Technology, 2007, 16, 881-885.	3.1	12
135	Examination of Substrate Surface Melting-Induced Splashing During Splat Formation in Plasma Spraying. Journal of Thermal Spray Technology, 2006, 15, 717-724.	3.1	33
136	Phase Formation of Nano-TiO ₂ Particles during Flame Spraying with Liquid Feedstock. Journal of Thermal Spray Technology, 2005, 14, 480-486.	3.1	32
137	Effects of annealing treatment on microstructure and photocatalytic performance of nanostructured TiO[sub 2] coatings through flame spraying with liquid feedstocks. Journal of Vacuum Science & Technology an Official Journal of the American Vacuum Society B, Microelectronics Processing and Phenomena, 2004, 22, 2364.	1.6	27
138	Title is missing!. Journal of Materials Science Letters, 2003, 22, 1499-1501.	0.5	6
139	Improving Adhesion Strength and Electrical Conductivity of Cold-Sprayed Al Deposit on Cu Substrate Through Friction-Stir-Processing. Journal of Thermal Spray Technology, 0, , 1.	3.1	0